INTERNATIONAL JOURNAL OF ADAPTIVE CONTROL AND SIGNAL PROCESSING
Int. J. Adapt. Control Signal Process. 2004; **18**:1–22 (DOI: 10.1002/acs.777)

Slope seeking: a generalization of extremum seeking

Kartik B. Ariyur[1,*,†,‡] and Miroslav Krstić[2,§]

[1] *Honeywell AES GN&C COE, MN65-2810, 3660 Technology Dr., Minneapolis, MN 55418, U.S.A.*
[2] *Department of MAE, University of California, San Diego, La Jolla, CA 92093-0411, U.S.A.*

SUMMARY

This work introduces slope seeking, a new idea for non-model based adaptive control. It involves driving the output of a plant to a value corresponding to a commanded slope of its reference-to-output map. To achieve this objective, we introduce a slope reference input into a sinusoidal perturbation-based extremum seeking scheme; derive a stability test for single parameter slope seeking, and then develop a systematic design algorithm based on standard linear SISO control methods to satisfy the stability test. We then extend the results to the multivariable case of gradient seeking. Finally, we illustrate near-optimal compressor operation under slope seeking feedback through a simulation study upon the well-known Moore–Greitzer model of compressor instability. Copyright © 2003 John Wiley & Sons, Ltd.

KEY WORDS: slope seeking; extremum seeking; compressor instability control

1. INTRODUCTION

We introduce in this work a new idea for non-model based adaptive control: *slope seeking involves driving the output of a plant to a value corresponding to a commanded slope of its reference-to-output map*. This is a generalization of the method of extremum seeking [1–6], that involves driving the plant output to an extremum of the reference-to-output map, i.e., a point on the reference-to-output map corresponding to a slope of zero. Motivations for the development of slope seeking are: problems where operation at the extremum of the plant reference-to-output map is susceptible to destabilization under finite disturbances, such as maximum pressure rise in deep hysteresis aeroengine compressors [7], antiskid braking for aircraft [8], minimum power demand formation flight [9], and problems in nuclear fusion where there is a need to stay away from the extremum (such as a maximal energy release condition) [10]. In fact, work on aircraft

*Correspondence to: Kartik B. Ariyur, Honeywell AES GN&C COE, MN65-2810, 3660 Technology Drive, Minneapolis, MN 55418, U.S.A.
† E-mail: kartik.ariyur@honeywell.com
‡ This work was performed while this author was with University of California, San Diego.
§ E-mail: krstic@ucsd.edu

Contract/grant sponsor: AFOSR
Contract/grant sponsor: ONR
Contract/grant sponsor: NSF

Published online 1 December 2003

Received 16 April 2003
Accepted 15 September 2003

antiskid control [8] used a slope set point in its extremum seeking loop. In all these problems, there is significant uncertainty in the models, and the set-points are unknown.

We supply the following results for enabling attainment of slope seeking feedback using sinusoidal perturbation:

(1) We formulate the problem for the case of the plant being a simple static map, the setting for classical extremum seeking schemes. We next formulate single parameter slope seeking for the general case where the map is embedded within dynamics with time-varying parameters as in recent works on extremum seeking [1, 2].
(2) We develop a stability test for single parameter slope seeking and provide systematic design guidelines using standard linear SISO control design methods to satisfy the stability test.
(3) We extend the results above to the multivariable case of gradient seeking.

The results obtained herein constitute a generalization of perturbation-based extremum seeking, which seeks a point of zero slope, to the problem of seeking a general slope. With a small modification, the results on convergence in extremum seeking and the design guidelines derived from [1] are extended to permit system operation at a point of arbitrary slope on the reference-to-output map. The modification involves setting a reference slope in the algorithm, which, in extremum seeking, is implicitly set to zero. The analysis is a simple extension of that used in proving output extremization in Reference [1]. For ease of understanding of the method, we present the result with slope seeking on a static map accompanied by an illustrative simulation. Finally, we apply slope seeking feedback in simulation to the well-known Moore–Greitzer model of compressor surge and stall and demonstrate: near-optimal compressor operation with only pressure sensing; robustness of the control to finite disturbances.

Section 2 presents slope seeking on a static map, Section 3 presents the analysis, and Section 4 the design algorithm for single parameter slope seeking for plants with dynamics; Section 5 supplies results on multiparameter gradient seeking. Section 6 presents a brief introduction to a parametrization of the well-known Moore–Greitzer [11] model for compressor surge and stall, and Section 7 illustrates near optimal compressor operation under slope seeking feedback.

2. SLOPE SEEKING ON A STATIC MAP

Figure 1 shows a basic slope seeking loop for a static map. We posit $f(\theta)$ of the form

$$f(\theta) = f^* + f'_{\text{ref}}(\theta - \theta^*) + \frac{f''}{2}(\theta - \theta^*)^2 \tag{1}$$

where f'_{ref} is the *commanded slope we want to operate at*, and $f'' > 0$. Any C^2 function $f(\theta)$ can be approximated locally by Equation (1). The assumption $f'' > 0$ is made without loss of generality. If $f'' < 0$, we just replace k ($k > 0$) in Figure 1with $-k$. The purpose of the algorithm is to make $\theta - \theta^*$ as small as possible, so that the output $f(\theta)$ is driven to its optimum f^*.

The perturbation signal $a \sin \omega t$ into the plant helps to give a measure of gradient information of the map $f(\theta)$. This is obtained by removing f^* from the output using the washout filter

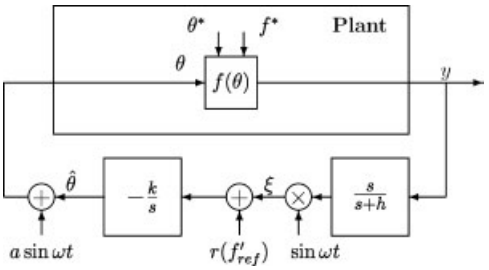

Figure 1. Basic slope seeking scheme.

$s/(s+h)$ $(h>0)$, and then demodulating the signal with $\sin \omega t$. In a sense, this can also be thought of as the online extraction of a Fourier coefficient. The input $r(f'_{\text{ref}})$ serves as a slope set point which is explicitly calculated below.

Output optimization: The following bare-bones result sums up the properties of the rudimentary slope seeking loop in Figure 1:

Theorem 2.1 (Slope Seeking)
For the system in Figure 1 the output error $y - f^*$ achieves local exponential convergence to an $O(a + 1/\omega)$ neighbourhood of the origin provided the perturbation frequency ω is sufficiently large, $1/(1 + L(s))$ is asymptotically stable, where

$$L(s) = \frac{kaf''}{2s} \tag{2}$$

and provided

$$r(f'_{\text{ref}}) = -\frac{af'_{\text{ref}}}{2} \operatorname{Re}\left\{\frac{\mathrm{j}\omega}{\mathrm{j}\omega + h}\right\} \tag{3}$$

We omit the proof as this result is subsumed in a more general result we prove in the following section. The result in Theorem 2.1 has the following salient features:

1. Like the analogous result on extremum seeking in Reference [1], it provides a linear stability test permitting design using linear SISO control tools.
2. Provided we know the sign of the second derivative f'' in the neighbourhood, we can create a feedback that drives the system to operate at a prespecified slope f'_{ref} of the input–output map; this is done exactly through setting the reference $r(f'_{\text{ref}}) = -(af'_{\text{ref}}/2)\operatorname{Re}\{\mathrm{j}\omega/\mathrm{j}\omega + h\}$.
3. Unlike the extremum seeking result, the convergence is only first order, i.e., $O(a + 1/\omega)$; this is because we are seeking a point of non-zero slope.

Simulation example: We present an example to illustrate the method proposed above. Simulation results are plotted with $f^*(t), \theta^*(t)$ in dotted lines and y, θ in solid lines. We use the static map $f(\theta) = f^* + 0.5(\theta - \theta^*) + (\theta - \theta^*)^2$, where $f^*(t) = 5.0$, and $\theta^* = 0.5$.

To satisfy the conditions in Theorem 2.1, we set $\omega = 5$ rad/s, $a = 0.05$, washout filter $s/(s + h)$ with $h = 5.0$, integrator gain $k = 10$, and slope setting $r(f'_{\text{ref}}) = -(af'_{\text{ref}}/2)\operatorname{Re}\{\mathrm{j}5/\mathrm{j}5 + 5\} =$

-0.00625 for operating at the slope $f'_{\text{ref}} = 0.5$. Substituting all parameters in Equation (2) we get

$$L(s) = \frac{1}{4s} \tag{4}$$

and attain stable slope seeking (Figure 2) through stability of $1/(1 + L(s))$. An extremum seeking design for the same plant with $r(f'_{\text{ref}}) = 0$, and other design parameters the same as for slope seeking, is shown in Figure 3 for comparison. Extremum seeking tracks a slope set point of zero, the minimum at $\theta = 0.25$ of the map $f(\theta)$ ($f(0.25) = 4.9375 < f(0.5) = 5$).

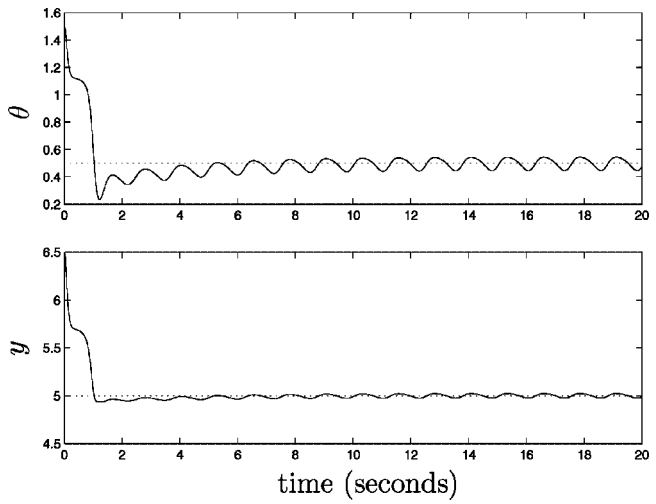

Figure 2. Slope seeking, $r(f'_{\text{ref}}) = -0.00625$.

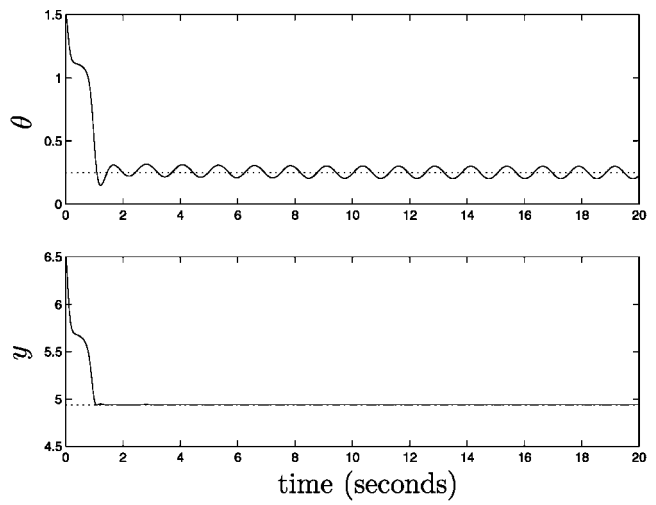

Figure 3. Extremum seeking, $r(f'_{\text{ref}}) = 0$.

3. GENERALIZED SINGLE PARAMETER SLOPE SEEKING

The generalized scheme differs from the rudimentary scheme of Figure 1 in the following ways: the map has time varying parameters and is embedded amidst linear dynamics; the slope seeking loop incorporates parameter dynamics for tracking parameter variations. Figure 4 shows the time-varying non-linear map embedded amidst linear dynamics along with the slope seeking loop. We posit $f(\theta)$ with time-varying parameters of the form

$$f(\theta) = f^*(t) + f'_{\text{ref}}(\theta - \theta^*(t)) + \frac{f''}{2}(\theta - \theta^*(t))^2 \tag{5}$$

where $f'' > 0$, and f'_{ref} is the commanded slope. Any C^2 function $f(\theta)$ can be approximated locally by Equation (5). The assumption $f'' > 0$ is made without loss of generality. If $f'' < 0$, we just replace $C_i(s)$ in Figure 4 with $-C_i(s)$. The purpose of the algorithm is to make $\theta - \theta^*$ as small as possible, so that the output $F_o(s)[f(\theta)]$ is driven to its optimum $F_o(s)[f^*(t)]$. n denotes measurement noise. Before proceeding to the analysis, we make the following assumptions:

Assumption 3.1

$F_i(s)$ and $F_o(s)$ are asymptotically stable and proper.

Assumption 3.2

$\mathscr{L}\{f^*(t)\} = \lambda_f \Gamma_f(s)$ and $\mathscr{L}\{\theta^*(t)\} = \lambda_\theta \Gamma_\theta(s)$ are strictly proper rational functions and poles of $\Gamma_\theta(s)$ that are not asymptotically stable are not zeros of $F_i(s)$.

This assumption forbids delta function variations in the map parameters and also the situation where tracking of the extremum is not possible.

Assumption 3.3

$C_o(s)/\Gamma_f(s)$ and $C_i(s)\Gamma_\theta(s)$ are proper.

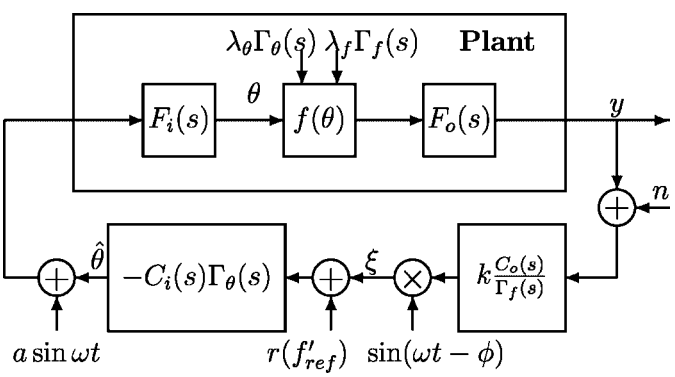

Figure 4. Generalized slope seeking.

This assumption ensures that the filters $C_o(s)/\Gamma_f(s)$ and $C_i(s)\Gamma_\theta(s)$ in Figure 4 can be implemented. Since $C_i(s)$ and $C_o(s)$ are at our disposal to design, we can always satisfy this assumption.

We introduce the following notation for use in analysis:

$$H_o(s) = k\frac{C_o(s)}{\Gamma_f(s)}F_o(s) \triangleq H_{osp}(s)\,H_{obp}(s) \triangleq H_{osp}(s)\,(1 + H_{obp}^{sp}(s)) \tag{6}$$

where $H_{osp}(s)$ denotes the strictly proper part of $H_o(s)$ and $H_{obp}(s)$ its biproper part, k is chosen to set

$$\lim_{s\to 0} H_{osp}(s) = 1 \tag{7}$$

We use two further assumptions from [1]:

Assumption 3.4

Let the smallest in absolute value among the real parts of all of the poles of $H_{osp}(s)$ be denoted by a. Let the largest among the moduli of all of the poles of $F_i(s)$ and $H_{obp}(s)$ be denoted by b. The ratio $M = a/b$ is sufficiently large.

The purpose of this assumption is to use a singular perturbation reduction of the output dynamics and provide the LTI SISO stability test of the theorem stated below. If the assumption were made upon the output dynamics $F_o(s)$ alone, the design would be restricted to plants with fast output dynamics $F_o(s)$. Hence, for generality in the design procedure, the assumption of fast poles is made upon the strictly proper factor $H_{osp}(s)$ of $H_o(s)$. Its purpose is to deal with the strictly proper part of $F_o(s)$. If we have slow poles in a strictly proper $F_o(s)$, *we can introduce a biproper* $C_o(s)/\Gamma_f(s)$ *with an equal number of fast poles* to permit analysis based design. For example, if

$$F_i(s) = \frac{1}{s+1} \quad \text{and} \quad F_o(s) = \frac{1}{(s+1)(2s+3)}$$

with constant f^* and θ^* (giving $\Gamma_\theta(s) = \Gamma_f(s) = 1/s$) we may set

$$C_o(s) = \frac{(s+4)}{(s+5)(s+6)}$$

and $k = 60$ to give

$$H_o(s) = \frac{C_o(s)}{\Gamma_f(s)}F_o(s) = \frac{60s\,(s+4)}{(s+1)(2s+3)(s+5)(s+6)}$$

We can factor the fast dynamics as

$$H_{osp}(s) = \frac{30}{(s+5)(s+6)}$$

and the slow biproper dynamics as

$$H_{obp}(s) = 1 + H_{obp}^{sp}(s) = 1 + \frac{1.5(s-1)}{(s+1)(s+1.5)}$$

This gives, in the terms of Assumption 3.4, the smallest pole in absolute value in $H_{\text{osp}}(s)$, $a = 5$, the largest of the moduli of poles in $F_i(s)$ and $H_{\text{obp}}(s)$ as $b = 1.5$, giving their ratio $M = a/b = 3.33$. The singular perturbation reduction reduces the fast dynamics $H_{\text{osp}}(s) = 30/(s+5)(s+6)$ to its unity gain, and we deal with stability of the reduced order model via the method of averaging to deduce stability conditions for the overall system in the theorem below.

Assumption 3.5

$H_i(s)$ is strictly proper.

This assumption is very easy to satisfy. Either $F_i(s)$ is strictly proper or, if it is biproper, one would choose $C_i(s)\Gamma_\theta(s)$ strictly proper. For example, if $F_i(s)$ is biproper and $\Gamma_\theta(s) = 1/s$, $C_i(s) = 1$ satisfies this assumption. The assumption is made only for the purpose of keeping the proof of the following theorem brief. The formation of a state space representation of the reduced order system for averaging becomes more intricate when $H_i(s)$ is biproper, because of the need to account for a factor of ω when time varying terms are differentiated, and this distracts from the main theme of the proof.

Output optimization. We first provide background for the result on slope seeking below. The following equations describe the single parameter slope seeking scheme in Figure 4:

$$y = F_{\text{o}}(s)\left[f^*(t) + f'_{\text{ref}}(\theta - \theta^*(t)) + \frac{f''}{2}(\theta - \theta^*(t))^2\right] \tag{8}$$

$$\theta = F_i(s)[a\sin(\omega t) - C_i(s)\Gamma_\theta(s)[\xi + r(f'_{\text{ref}})]] \tag{9}$$

$$\xi = \sin(\omega t - \phi)\, k\, \frac{C_{\text{o}}(s)}{\Gamma_f(s)}[y + n] \tag{10}$$

For the purpose of analysis, we define the tracking error $\tilde{\theta}$ and output error $\tilde{y}$:

$$\tilde{\theta} = \theta^*(t) - \theta + \theta_0 \tag{11}$$

$$\theta_0 = F_i(s)[a\sin(\omega t)] \tag{12}$$

$$\tilde{y} = y - F_{\text{o}}(s)[f^*(t)] \tag{13}$$

In terms of these definitions, we can restate the goal of slope seeking as driving output error $\tilde{y}$ to a small value by tracking $\theta^*(t)$ with θ. With the present method, we cannot drive $\tilde{y}$ to zero because of the sinusoidal perturbation θ_0 . We are now ready for our single parameter result:

Theorem 3.1 (Slope Seeking)
For the system in Figure 4, under Assumptions 3.1–3.5, the output error $\tilde{y}$ achieves local exponential convergence to an $O(a + \delta)$ neighbourhood of the origin, where $\delta = 1/\omega + 1/M$, provided $n = 0$ and:

(1) Perturbation frequency ω is sufficiently large, and $\pm j\omega$ is not a zero of $F_i(s)$.
(2) Zeros of $\Gamma_f(s)$ that are not asymptotically stable are also zeros of $C_{\text{o}}(s)$.
(3) Poles of $\Gamma_\theta(s)$ that are not asymptotically stable are not zeros of $C_i(s)$.

(4) $C_o(s)$ and $1/(1+L(s))$ are asymptotically stable, where

$$L(s) = \frac{af''}{4}\,\mathrm{Re}\{e^{j\phi}F_i(j\omega)\}H_i(s) \tag{14}$$

$$H_i(s) = C_i(s)\Gamma_\theta(s)F_i(s) \tag{15}$$

(5) $r(f'_{\mathrm{ref}}) = -af'_{\mathrm{ref}}/2\,\mathrm{Re}\{e^{-j\phi}H_o(j\omega)F_i(j\omega)\}$.

Proof

Using $n = 0$ and substituting Equations (9) and (12) in Equation (11) yields

$$\tilde{\theta} = \theta^* + H_i(s)[\xi + r(f'_{\mathrm{ref}})] \tag{16}$$

Further, substitution for ξ from Equation (10) and for y from Equation (8) yields

$$\tilde{\theta} = \theta^* + H_i(s)\left[\sin(\omega t - \phi)H_o(s)\left[f^* + f'_{\mathrm{ref}}(\theta - \theta^*) + \frac{f''}{2}(\theta - \theta^*)^2\right] + r\,(f'_{\mathrm{ref}})\right] \tag{17}$$

Using $\theta - \theta^* = \theta_0 - \tilde{\theta}$ from Equation (11), we get

$$\begin{aligned}\tilde{\theta} &= \theta^* + H_i(s)\left[\sin(\omega t - \phi)H_o(s)\left[f^* + f'_{\mathrm{ref}}(\theta_0 - \tilde{\theta}) + \frac{f''}{2}(\theta_0 - \tilde{\theta})^2\right] + r\,(f'_{\mathrm{ref}})\right] \\ &= \theta^* + H_i(s)\left[\sin(\omega t - \phi)H_o(s)\left[f^* + f'_{\mathrm{ref}}\theta_0 - f'_{\mathrm{ref}}\tilde{\theta} + \frac{f''}{2}(\theta_0^2 - 2\theta_0\tilde{\theta} + \tilde{\theta}^2)\right] + r\,(f'_{\mathrm{ref}})\right]\end{aligned} \tag{18}$$

We drop the higher order term[¶] $\tilde{\theta}^2$ and simplify the expression in Equation (18) using Lemmas A1, A2, Assumptions 3.1–3.3 and asymptotic stability of $C_o(s)/\Gamma_f(s)$ and $C_o(s)$:

$$\begin{aligned}\sin(\omega t - \phi)H_o(s)[f^*(t)] &= \lambda_f \sin(\omega t - \phi)\mathscr{L}^{-1}(H_o(s)\Gamma_f(s)) \\ &= \sin(\omega t - \phi)(\varepsilon^{-t}) = \varepsilon^{-t}\end{aligned} \tag{19}$$

$$\sin(\omega t - \phi)H_o(s)[\theta_0^2] = C_1 a^2 \sin(\omega t + \mu_1) + C_2 a^2 \sin(3\omega t + \mu_2) + \varepsilon^{-t} \tag{20}$$

$$\begin{aligned}\sin(\omega t - \phi)H_o(s)[f'_{\mathrm{ref}}\theta_0] = \frac{af'_{\mathrm{ref}}}{2}&(\mathrm{Re}\{e^{-j\phi}H_o(j\omega)F_i(j\omega)\} \\ &- \mathrm{Re}\{e^{j(2\omega t - \phi)}H_o(j\omega)F_i(j\omega)\}) + \varepsilon^{-t}\end{aligned} \tag{21}$$

where C_1, C_2, μ_1, μ_2 are constants (these can be determined from the frequency response of $H_o(s)$), and ε^{-t} denotes exponentially decaying terms. Hence, after substituting Equations (19)–(21) in Equation (18) we can write the linearization of Equation (18) as

$$\tilde{\theta} = \theta^* + H_i(s)[\sin(\omega t - \phi)H_o(s)[-f'_{\mathrm{ref}}\tilde{\theta} - f''\theta_0\tilde{\theta}] + \omega(t) + \varepsilon^{-t}] \tag{22}$$

[¶] This is justified by Lyapunov's first method, as we have already written the system in terms of error variable $\tilde{\theta}$ thus transforming the problem to stability of the origin. As in the proof of Theorem 2.1 in Reference [1], this is responsible for the result in the theorem being local.

$$\omega(t) = a^2 \frac{f''}{2}[C_1 \sin(\omega t + \mu_1) + C_2 \sin(3\omega t + \mu_2)]$$

$$+ \frac{a f'_{\text{ref}}}{2} \text{Re}\{e^{j(2\omega t - \phi)} H_o(j\omega) F_i(j\omega)\} \tag{23}$$

where we have used

$$r(f'_{\text{ref}}) = -\frac{a f'_{\text{ref}}}{2} \text{Re}\{e^{-j\phi} H_o(j\omega) F_i(j\omega)\}$$

Applying the reduction of $H_o(s)$ from Assumption 3.4 and Lemmas A1, A2 in succession to the terms containing $2\theta_0\tilde{\theta}$ and $f'_{\text{ref}}\tilde{\theta}$ in Equation (22), we get[‖]

$$H_i(s)[\sin(\omega t - \phi) H_o(s)[-f''\theta_0\tilde{\theta} - f'_{\text{ref}}\tilde{\theta}]]$$

$$= H_i(s)[\sin(\omega t - \phi)(1 + H^{\text{sp}}_{\text{obp}}(s))[-f''\theta_0\tilde{\theta} + f'_{\text{ref}}\tilde{\theta}]] \tag{24}$$

$$= \mathscr{T}[\tilde{\theta}] - L(s)[\tilde{\theta}] - \mathscr{S}[\tilde{\theta}] + H_i(s)[\sin(\omega t - \phi) v_0(t)] \tag{25}$$

where

$$L(s)[\tilde{\theta}] = \frac{a f''}{2} H_i(s)[\text{Re}\{e^{j\phi} F_i(j\omega)[\tilde{\theta}]\}] \tag{26}$$

$$\mathscr{T}[\tilde{\theta}] = \frac{a f''}{2} H_i(s)[\text{Re}\{e^{j(2\omega t - \phi)} F_i(j\omega)[\tilde{\theta}]\}] \tag{27}$$

$$\mathscr{S}[\tilde{\theta}] = f'_{\text{ref}} H_i(s)[\sin(\omega t - \phi)\tilde{\theta}] \tag{28}$$

$$v_0(t) = H^{\text{sp}}_{\text{obp}}(s)[-f'' \text{Im}\{a F_i(j\omega) e^{j\omega t}\}\tilde{\theta} + f'_{\text{ref}}\tilde{\theta}] \tag{29}$$

Finally, substituting Equation (25) in Equation (22), and moving the terms linear in $\tilde{\theta}$ to the left-hand side, we get

$$(1 + L(s) - \mathscr{T} + \mathscr{S})[\tilde{\theta}] - H_i(s)[\sin(\omega t - \phi) v_0(t)]$$

$$= \theta^* + H_i(s)[\omega(t) + \varepsilon^{-t}] \tag{30}$$

We now divide both sides of Equation (30) with $1 + L(s)$ and rewrite it as

$$\tilde{\theta} - Y_i(s)[a f''/2 \text{Re}\{e^{j(2\omega t - \phi)}\tilde{\theta}\} + a f'_{\text{ref}} \sin(\omega t - \phi)\tilde{\theta} + \sin(\omega t - \phi) v_0(t)]$$

$$= \frac{1}{1 + L(s)}[\theta^*] + Y_i(s)[w(t) + \varepsilon^{-t}] \tag{31}$$

[‖] Note that Equation (25) contains an additional term of the form $H_i(s)[\sin(\omega t - \phi) H_o(s)[\varepsilon^{-t}\tilde{\theta}]]$ which comes from ε^{-t} in $\theta_0(t) = a \text{Im}\{F_i(j\omega) e^{j\omega t}\} + \varepsilon^{-t}$. We drop this term from subsequent analysis because it does not affect closed-loop stability or asymptotic performance. It can be accounted for in three ways. One is to perform averaging over an infinite time interval in which all exponentially decaying terms disappear. The second way is to treat $\varepsilon^{-t}\tilde{\theta}$ as a vanishing perturbation via Corollary 5.4 in Reference [12], observing that ε^{-t} is integrable. The third way is to express ε^{-t} in state space format and let $\varepsilon^{-t}\theta$ be dominated by other terms in a local Lyapunov analysis.

where $Y_i(s) = H_i(s)/(1 + L(s)) = \text{num}\{Y_i(s)\}/\text{num}\{1 + L(s)\}$ is asymptotically stable because the poles of $H_i(s)$ are cancelled by zeros of $1/(1 + L(s))$, and $1/(1 + L(s))$ is asymptotically stable. By noting also that zeros in $1/(1 + L(s))$ cancel poles in $\theta^*(s) = \lambda_\theta \Gamma_\theta(s)$, and using asymptotic stability of $1/(1 + L(s))$, we get

$$\tilde{\theta} - Y_i(s)[af''/2\text{Re}\{e^{j(2\omega t-\phi)}\tilde{\theta}\} + af'_{\text{ref}} \sin(\omega t - \phi)\tilde{\theta} + \sin(\omega t - \phi)v_0(t)]$$

$$= \varepsilon^{-t} + Y_i(s)[w(t)] \tag{32}$$

Now, $Y_i(s)$ is strictly proper, and can therefore be written as $Y_i(s) = 1/(s + p_0)Y'_i(s)$, where $Y'_i(s)$ is proper. In terms of their partial fraction expansions, we can write $Y'_i(s) = A_0 + \sum_{k=1}^{n} A_k/(s + p_k)$, and $H^{\text{sp}}_{\text{obp}}(s) = \sum_{j=1}^{m} B_j/(s + p_j)$. Multiplying both sides of Equation (32) with $s + p_0$ and using the partial fraction expansions, we get

$$\tilde{\theta} + p_0\tilde{\theta} - A_0(u_0(t) + \sin(\omega t - \phi)v_0(t) - w(t))$$

$$- \sum_{k=1}^{n} (u_k(t) + v_k(t) - w_k(t)) = \varepsilon^{-t} \tag{33}$$

$$u_0(t) = af''/2\text{Re}\{e^{j(2\omega t-\phi)}\tilde{\theta}\} + af'_{\text{ref}} \sin(\omega t - \phi)\tilde{\theta}$$

$$u_k(t) = \frac{A_k}{s + p_k}[u_0(t)], \quad v_k(t) = \frac{A_k}{s + p_k}[\sin(\omega t - \phi)v_0(t)]$$

$$w_k(t) = \frac{A_k}{s + p_k}[w(t)]$$

$$v_0(t) = \sum_{j=1}^{m} v_{1j}(t), \quad v_{1j}(t) = \frac{B_j}{s + p_j}[-f'' \,\text{Im}\{aF_i(j\omega)e^{j\omega t}\}\tilde{\theta} + f'_{\text{ref}}\tilde{\theta}] \tag{34}$$

We can write the system of linear time varying differential equations above in the state-space form:

$$\dot{\mathbf{x}} = A(t)\mathbf{x} + A_{12}\mathbf{x}_e + Bw(t); \quad \tilde{\theta} = x_1 \tag{35}$$

$$\dot{\mathbf{x}}_e = A_e\mathbf{x}_e \tag{36}$$

Equation (36) is a representation for the ε^{-t}. We get Equations (35) and (36) into the standard form for averaging by using the transformation $\tau = \omega t$, and then averaging the right-hand side of the equations w.r.t. time from 0 to $T = 2\pi/\omega$, i.e., $1/T \int_0^T (\cdot)\, d\tau$ treating states $\mathbf{x}, \mathbf{x}_e$ as constant to get:

$$\frac{d\mathbf{x}_{\text{av}}}{d\tau} = \frac{1}{\omega}(A_{\text{av}}\mathbf{x}_{\text{av}} + A_{12}\mathbf{x}_{e\text{av}}), \quad \tilde{\theta}_{\text{av}} = x_{1\text{av}} \tag{37}$$

$$\frac{d\mathbf{x}_{e\text{av}}}{d\tau} = \frac{1}{\omega}A_e\mathbf{x}_{e\text{av}} \tag{38}$$

which is a state-space representation of the system in the $\tau = \omega t$ time-scale, and $A_{\text{av}} = 1/T \int_0^T (A(\tau))\, \mathrm{d}\tau$. This gives

$$\dot{\tilde{\theta}}_{\text{av}} + p_0 \tilde{\theta}_{\text{av}} - \sum_{k=1}^{n} (u_{k,\text{av}} + v_{k,\text{av}} - w_{k,\text{av}}) = \varepsilon^{-t} \tag{39}$$

$$\dot{u}_{k,\text{av}} + p_k u_{k,\text{av}} = 0, \quad \dot{v}_{k,\text{av}} + p_k v_{k,\text{av}} = 0, \quad \dot{w}_{k,\text{av}} + p_k w_{k,\text{av}} = 0$$

$$v_{0,\text{av}} = \sum_{j=1}^{m} v_{1j,\text{av}}, \;\; \dot{v}_{1j,\text{av}} + p_j v_{1j,\text{av}} = B_j f'_{\text{ref}} \tilde{\theta}_{\text{av}} \tag{40}$$

in the original time-scale. As all of the poles p_k for all k and p_j for all j are asymptotically stable (from asymptotic stability of $H_{\text{o}}(s)$ and $1/(1 + L(s))$), all of the terms on the right-hand side of Equation (39) for $\tilde{\theta}_{\text{av}}$ are exponentially decaying, i.e., we have

$$\dot{\tilde{\theta}}_{\text{av}} + p_0 \tilde{\theta}_{\text{av}} = \varepsilon^{-t} \tag{41}$$

which decays to zero because p_0, a pole of $1/(1 + L(s))$ is asymptotically stable. Hence, by a standard averaging theorem such as Theorem 8.3 in Reference [12], we see that if $\omega, a, \phi, C_i(s)$ and $C_{\text{o}}(s)$ are such that $1/(1 + L(s))$ is asymptotically stable, and ω is sufficiently large relative to other parameters of the state-space representation, solutions starting from small initial conditions converge exponentially to a periodic solution in an $O(1/\omega)$ neighbourhood of zero. Hence, $\tilde{\theta}(t)$ goes to a periodic solution $\tilde{\theta}_{\text{per}}(t) = O(1/\omega)$. We now proceed to put the system in the standard form for singular perturbation analysis through making the transformation $\delta\tilde{\theta} = \tilde{\theta}(t) - \tilde{\theta}_{\text{per}}(t)$ in the unreduced linearized system in Equation (22) and get:

$$\delta\tilde{\theta} + \tilde{\theta}_{\text{per}}(t) = \theta^* + H_i(s)[\sin(\omega t - \phi)[y'_{\text{osp}}] + w(t) + \varepsilon^{-t}] \tag{42}$$

$$y'_{\text{osp}} = (1 + H^{\text{sp}}_{\text{obp}}(s))[y_{\text{osp}}]$$

$$y_{\text{osp}} = H_{\text{osp}}(s)[(f''\theta_0 - f'_{\text{ref}})(\delta\tilde{\theta} + \tilde{\theta}_{\text{per}})] \tag{43}$$

By linearity of the system described by Equations (42), (36), we have that the reduced order model in the new co-ordinates (replacing $H_{\text{osp}}(s)$ with its unity static gain) is given by

$$\delta\tilde{\theta} = H_i(s)[\sin(\omega t - \phi)[y'_{\text{osp}}]]$$

$$y'_{\text{osp}} = -(1 + H^{\text{sp}}_{\text{obp}}(s))[(f''\theta_0 + f'_{\text{ref}})\delta\tilde{\theta}] \tag{44}$$

which has the state-space representation

$$\dot{\mathbf{x}} = A(t)\mathbf{x}; \quad \delta\tilde{\theta} = x_1 \tag{45}$$

where $A(t)$ is the same as in Equation (35). Hence $\delta\tilde{\theta}$ converges exponentially to the origin. This shows that the reduced order model is exponentially stable. From exponential stability of $H_{\text{osp}}(s)$, we have exponential stability of the boundary layer model

$$\frac{\mathrm{d}\mathbf{y}}{\mathrm{d}\tau} = \mathbf{A}_{\text{osp}}\mathbf{y} \tag{46}$$

where $(\mathbf{A}_{\text{osp}}, \mathbf{B}_{\text{osp}}, \mathbf{C}_{\text{osp}})$ is a state-space representation of $H_{\text{osp}}(s)$, with $\mathbf{C}_{\text{osp}}\mathbf{A}_{\text{osp}}^{-1}\mathbf{B}_{\text{osp}} = 1$ from Equation (6). Hence, by the Singular Perturbation Lemma A3, we have that in the overall unreduced system in Equations (42) and (43), the solution converges to an $O(1/M)$

neighbourhood of the origin. Hence, $\delta\tilde{\theta}(t)$ converges to a $O(1/M)$ neighbourhood of the origin. Therefore, $\tilde{\theta}$ converges exponentially to a $O(1/\omega) + O(1/M) = O(\delta)$ neighbourhood of the origin. Further, the output error $\tilde{y}$ decays to $O(a+\delta)$:

$$\begin{aligned}\tilde{y} &= F_o(s)\left[f'_{\text{ref}}(\theta-\theta^*) + \frac{f''}{2}(\theta-\theta^*)^2\right] \\ &= F_o(s)\left[f'_{\text{ref}}(\tilde{\theta}-\theta_0) + \frac{f''}{2}(\tilde{\theta}-\theta_0)^2\right] = O(a+\delta)\end{aligned} \tag{47}$$

dropping second-order terms, which completes the proof.

The output error $\tilde{y}$ converges to an $O(a+1/\omega)$ neighbourhood of the origin. Thus, the deviation of the output from the desired output will be larger than that achievable in extremum seeking, where we track a point on the map with zero first derivative. We next provide rigorous design guidelines that satisfy the conditions of Theorem 3.1. We now note that *for* $r(f'_{\text{ref}}) = 0$, *the slope seeking scheme reduces to the extremum seeking scheme in Reference* [1].

4. COMPENSATOR DESIGN

In the design guidelines that follow, we set $\phi = 0$ which can be used separately for fine-tuning.

Algorithm 4.1 (Single Parameter Slope Seeking)

(1) Select the perturbation frequency ω sufficiently large. Also, ω should not equal any frequency in noise.
(2) Set perturbation amplitude a so as to obtain small steady-state output error $\tilde{y}$.
(3) Design $C_o(s)$ asymptotically stable, with zeros of $\Gamma_f(s)$ that are not asymptotically stable as its zeros, and such that $C_o(s)/\Gamma_f(s)$ is proper. In the case where dynamics in $F_o(s)$ are slow and strictly proper, use as many fast poles in $C_o(s)$ as the relative degree of $F_o(s)$, and as many zeros as needed to have zero relative degree of the slow part $H_{\text{obp}}(s)$ to satisfy Assumption 3.4.
(4) Design $C_i(s)$ by any linear SISO design technique such that it does not include poles of $\Gamma_\theta(s)$ that are not asymptotically stable as its zeros, $C_i(s)\Gamma_\theta(s)$ is proper, and $1/(1+L(s))$ is asymptotically stable.
(5) Set $r(f'_{\text{ref}}) = -af'_{\text{ref}}/2\,\text{Re}\{e^{-j\phi}H_o(j\omega)F_i(j\omega)\}$.

Steps $1,\ldots,4$ are discussed fully in Reference [1]. A point that we note here is that simplification of the design for $C_i(s)$ is achieved by setting $\phi = -\angle(F_i(j\omega))$, and obtaining

$$L(s) = \frac{af''|F_i(j\omega)|}{4}H_i(s)$$

The setting of $r(f'_{\text{ref}})$ requires knowledge of the frequency response of $F_i(s)$ and $F_o(s)$ at ω. We note here that seeking large slopes is difficult because $\tilde{y}$ will be correspondingly large from Equation (47).

Convergence of the scheme requires asymptotic stability of $1/(1+L(s))$, and this requires knowledge of the second derivative f'' of the map at θ^*, or robustness to a range of values of f''. This is dealt with in Reference [1].

5. MULTIPARAMETER GRADIENT SEEKING

The results on multiparameter extremum seeking presented in Reference [1] can be extended to gradient seeking through setting reference inputs in each of the parameter tracking loops. Figure 5 shows the multiparameter gradient seeking scheme with reference inputs r_p ($r_p = 0$ in each loop corresponds to the multiparameter extremum seeking scheme in Reference [1]). Analogous to the single parameter case in Section 3, we let $f(\theta)$ be a function of the form

$$f(\theta) = f^*(t) + \mathbf{J}^{\mathrm{T}}(\theta - \theta^*(t)) + (\theta - \theta^*(t))^{\mathrm{T}}\mathbf{P}(\theta - \theta^*(t)) \tag{48}$$

where $\mathbf{P}_{l\times l} = \mathbf{P}^{\mathrm{T}}, \theta = [\theta_1 \dots \theta_l]^{\mathrm{T}}$, $\theta^*(t) = [\theta_1^*(t) \dots \theta_l^*(t)]^{\mathrm{T}}$, $\mathscr{L}\{\theta^*(t)\} = \Gamma_\theta(s) = [\lambda_1\Gamma_{\theta 1}(s), \dots, \lambda_l\Gamma_{\theta l}(s)]^{\mathrm{T}}$, $\mathscr{L}\{f^*(t)\} = \lambda_f\Gamma_f(s)$, and $\mathbf{J} = [J_1, J_2, \dots, J_l]$ is the *commanded gradient*. Any twice differentiable vector function $f(\theta)$ can be approximated by Equation (48). As in multiparameter extremum seeking, the broad principle of using m frequencies for identification/tracking of $2m$ parameters applies; but for simplicity of presentation, we only present the case where a separate forcing frequency is used in each parameter tracking loop, i.e., we use forcing frequencies $\omega_1 < \omega_3 < \cdots < \omega_l$. We make assumptions identical to those made to prove Theorem 3.1 in Reference [1]:

Assumption 5.1

$\mathbf{F}_i(s) = [F_{i1}(s) \dots F_{il}(s)]^{\mathrm{T}}$ and $F_{\mathrm{o}}(s)$ are asymptotically stable and proper.

Assumption 5.2

$\Gamma_\theta(s)$ and $\Gamma_f(s)$ are strictly proper.

Assumption 5.3

$C_{ip}(s)\Gamma_{\theta p}(s)$ and $C_{\mathrm{op}}(s)/\Gamma_f(s)$ are proper for all $p = 1, 2, \dots, l$.

Assumption 5.4 (Rotea [4])
$\omega_p + \omega_q \neq \omega_r$ for any $p, q, r = 1, 2, \dots, l$.

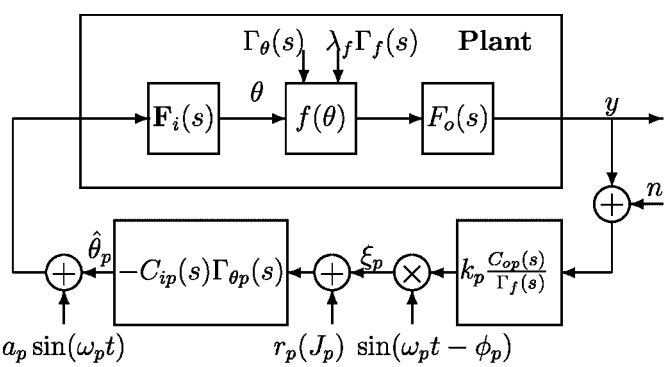

Figure 5. Multiparameter gradient seeking with $p = 1, 2, \dots, l$.

As with multiparameter extremum seeking in Reference [1], we introduce the following notation for the next assumption:

$$H_{\mathrm{op}}(s) = k_p \frac{C_{\mathrm{op}}(s)}{\Gamma_f(s)} F_{\mathrm{o}}(s) \triangleq H_{\mathrm{osp},p}(s) H_{\mathrm{obp},p}(s)$$
$$\triangleq H_{\mathrm{osp},p}(s)(1 + H^{\mathrm{sp}}_{\mathrm{obp},p}(s)) \tag{49}$$

$$\lim_{s\to 0} H_{\mathrm{osp},p}(s) = 1$$

where $H_{\mathrm{osp},p}(s)$ denotes the strictly proper part of $H_{\mathrm{op}}(s)$ and $H_{\mathrm{obp},p}(s)$ its biproper part, k_p, $p = 1, \ldots, l$ is chosen to normalize the static gain of $H_{\mathrm{osp},p}(s)$ to unity.

Assumption 5.5

Let the smallest in absolute value among the real parts of all of the poles of $H_{\mathrm{osp},p}(s)$ for all p be denoted by a. Let the largest among the moduli of all of the poles of $F_{ip}(s)$ and $H_{\mathrm{obp},p}(s)$ for all p, be denoted by b. The ratio $M = a/b$ is sufficiently large.

Theorem 5.1 (Multiparameter Gradient Seeking)
For the system in Figure 5, under Assumptions 5.1–5.5, the output y achieves local exponential convergence to an $O(\sum_{p=1}^{l} a_p + \Delta)$ neighbourhood of $F_{\mathrm{o}}(s)[f^*(t)]$ provided $n = 0$ and:

(1) Perturbation frequencies $\omega_1 < \omega_2 < \cdots < \omega_l$ are rational, sufficiently large, and $\pm \mathrm{j}\omega_p$ is not a zero of $F_{ip}(s)$.
(2) Zeros of $\Gamma_f(s)$ that are not asymptotically stable are also zeros of $C_{\mathrm{op}}(s)$ for all $p = 1, \ldots, l$.
(3) Poles of $\Gamma_{\theta p}(s)$ that are not asymptotically stable are not zeros of $C_{ip}(s)$, for any $p = 1, \ldots, l$.
(4) $C_{\mathrm{op}}(s)$ are asymptotically stable for all $p = 1, \ldots, l$ and $1/\det(\mathbf{I}_l + \mathbf{X}(s))$ is asymptotically stable, where $X_{pq}(s)$ denote the elements of $\mathbf{X}(s)$ and

$$X_{pq}(s) = P_{pq} a_p L_p(s), \quad q = 1, \ldots, l \tag{50}$$

$$L_p(s) = \tfrac{1}{4} H_{ip}(s)\, \mathrm{Re}\{\mathrm{e}^{\mathrm{j}\phi_p} F_{ip}(\mathrm{j}\omega_p)\} \tag{51}$$

where $H_{ip}(s) = C_{ip}(s)\Gamma_{\theta p}(s)F_{ip}(s)$ and $\Delta = 1/\omega + 1/M$.

(5) The reference is chosen as

$$r_p(J_p) = -\frac{a_p J_p}{2} \mathbf{Re}\{\mathrm{e}^{-\mathrm{j}\phi_p} H_{\mathrm{op}}(\mathrm{j}\omega_p) F_{ip}(\mathrm{j}\omega_p)\}, \quad p = 1, \ldots, 1$$

The proof is a simple extension of the proof of Theorem 3.1 in Reference [1]. Additional terms produced by the gradient term in Equation (48) are handled without any difficulty by the method of averaging. The key point to note in this result is that *the greater the number of parameters*, *the poorer the convergence*. Furthermore, the design guidelines in Reference [1] apply to gradient seeking with the added specification of the components of the gradient, $r_1(J_1), r_2(J_2), \ldots, r_l(J_l)$ by Theorem 5.1.

6. COMPRESSOR STALL AND SURGE: THE MOORE–GREITZER MODEL

Most experimentally validated control designs for compressors (see Reference [7]) have been based upon the well-known three state non-linear model of Moore and Greitzer [11]. It is a Galerkin approximation of a higher order PDE model and the simplest model that adequately describes the basic dynamics of rotating stall and surge:

$$\dot{R} = \sigma R \mathscr{F}(R, \Phi) \tag{52}$$

$$\dot{\Phi} = -\Psi + \mathscr{G}(R, \Phi) \tag{53}$$

$$\dot{\Psi} = \frac{1}{\beta^2}(\Phi - \Phi_T) \tag{54}$$

where the functions $\mathscr{F}(R, \Phi)$ and $\mathscr{G}(R, \Phi)$ are given by

$$\mathscr{F}(R, \Phi) = \frac{1}{3\pi\sqrt{R}} \int_0^{2\pi} \Psi_C(\Phi + 2\sqrt{R}\sin\theta)\sin\theta \, d\theta \tag{55}$$

$$\mathscr{G}(R, \Phi) = \frac{1}{2\pi} \int_0^{2\pi} \Psi_C(\Phi + 2\sqrt{R}\sin\theta) \, d\theta \tag{56}$$

The quantities appearing in this model are listed in Table I, with $R = (A/2)^2$. The function $\Psi_C(\Phi)$ is the steady-state annulus-averaged compressor characteristic. The throttle flow Φ_T is related to the pressure rise Ψ through the throttle characteristic

$$\Psi = \frac{1}{\gamma^2}(1 + \Phi_{C0} + \Phi_T)^2 \tag{57}$$

where γ is the throttle opening. We optimize performance by controlling γ in the next section.

Table I. Notation in the Moore–Greitzer model.

$\Phi = \hat{\Phi}/W - 1 - \Phi_{C0}$	$\hat{\Phi}$—annulus-averaged flow coefficient W—compressor characteristic semi-width
$\Psi = \hat{\Psi}/H$	$\hat{\Psi}$—plenum pressure rise H—compressor characteristic semi-height
$A = \hat{A}/W$	$\hat{A}$—rotating stall amplitude
Φ_T	Mass flow through the throttle/$W - 1$
θ	Angular (circumferential) position
$\beta = \frac{2H}{W}B$	B—Greitzer stability parameter
$\sigma = \frac{3l_c}{m + \mu}$	l_c—Effective length of inlet duct normalized by compressor radius m—Moore expansion parameter μ—Compressor inertia within blade passage
$t = \frac{H}{Wl_c}\hat{t}$	$\hat{t}$ = (actual time)× (rotor angular velocity)

The ε-MG3 model parametrization: The following parametrization of compressor characteristic $\Psi_C(\Phi)$ proposed in Reference [7] permits capturing the qualitative properties of a large variety of compressors:

$$\Psi_C(\Phi) = \Psi_{C0} + 1 + (1-\varepsilon)\left(\frac{3}{2}\Phi - \frac{1}{2}\Phi^3\right) + \varepsilon\frac{2\Phi}{1+\Phi^2} \tag{58}$$

where $\varepsilon \in [0,1]$. Evaluation of the integrals in Equations (52)–(54) with the characteristic in Equation (58) leads to the following differential equations [7]:

$$\begin{aligned}\dot{R} = \sigma\Bigg\{&(1-\varepsilon)R(1-\phi^2-R) + \frac{2\varepsilon}{3}\Bigg[1 - \frac{1}{\sqrt{2}[(\phi^2-4R-1)^2+4\Phi^2]^{1/2}} \\ &\times ((((\Phi^2-1)(\Phi^2-4R-1)+4\Phi^2)^2 + 64\Phi^2R^2)^{1/2} \\ &+ (\Phi^2-1)(\Phi^2-4R-1)+4\Phi^2)^{1/2}\Bigg]\Bigg\}\end{aligned} \tag{59}$$

$$\begin{aligned}\dot{\Phi} = &-\Psi + \Psi_{C0} + 1 + (1-\varepsilon)\left(\frac{3}{2}\Phi - \frac{1}{2}\Phi^3 - 3\Phi R\right) \\ &+ \varepsilon\frac{\sqrt{2}\,\mathrm{sgn}(\Phi)}{[(\Phi^2-4R-1)^2+4\Phi^2]^{1/2}}\{[(\Phi^2-4R-1)^2+4\Phi^2]^{1/2} \\ &+ (\Phi^2-4R-1)\}^{1/2}\end{aligned} \tag{60}$$

$$\dot{\Psi} = \frac{1}{\beta^2}(\Phi - \Phi_T) \tag{61}$$

We refer to this model as the ε-MG3 model. Note that, even though (53) contains sgn(Φ), this equation is not discontinuous because the term multiplied by sgn(Φ) vanishes at $\Phi = 0$ for all values of R. There are two sets of equilibria of the model in Equations (59)–(61). The no-stall equilibria are:

$$\begin{bmatrix} R \\ \Phi \\ \Psi \end{bmatrix}_e = \begin{bmatrix} 0 \\ \Phi_0 \\ \Psi_C(\Phi_0) \end{bmatrix}, \quad \Phi_0 \in \mathbb{R} \tag{62}$$

The stall equilibra are:

$$\begin{bmatrix} R \\ \Phi \\ \Psi \end{bmatrix}_e = \begin{bmatrix} R_0 \\ \Phi_{R\pm}(R_0) \\ \Psi_{R\pm}(R_0) \end{bmatrix}, \quad R_0 \in [0, \bar{R}] \tag{63}$$

The functions $\Phi_{R+}(R)$ and $\Phi_{R-}(R)$ are obtained as solutions of (59) with $\dot{R} = \sigma R\mathscr{F}(R,\Phi) = 0$ and $R \neq 0$. Note that since $\mathscr{F}(R,\Phi)$ in (59) is a function of Φ^2, we get two solutions $\Phi_{R-}(R) = -\Phi_{R+}(R)$. The functions $\Psi_{R+}(R)$ and $\Psi_{R-}(R)$ are obtained as solutions of (61) with $\dot{\Phi} = -\Psi + \mathscr{G}(R,\Phi) = 0$, that is, by substituting $\Phi = \Phi_{R\pm}(R)$ into $\Psi = \mathscr{G}(R,\Phi)$.

7. NEAR OPTIMAL COMPRESSOR OPERATION WITH SLOPE SEEKING FEEDBACK

For the purpose of our study, we consider a three-stage compressor considered in Reference [7] with parameters $\Psi_{C0} = 0.72$, $\Phi_{C0} = 0$ and $\sigma = 4$. Furthermore we choose the low speed case of $\beta = 0.71$ from [7]. Figures 6 and 7 show the bifurcation diagrams for the compressor for $\varepsilon = 0$ and 0.9, respectively; the solid lines showing stable equilibria and the dotted lines showing unstable equilibria.

The performance objective for compressors is to maximize the pressure rise Ψ with respect to the mass flow Φ without entering stall or surge instabilities. But as seen from the Ψ versus γ diagrams in Figures 6 and 7, the point of maximum pressure rise is directly above a stable stall equilibrium, and the stable high pressure branch ends at the maximum. The stall branch comes very deep under the high pressure branch in the case when $\varepsilon = 0.9$; showing a deep hysteresis characteristic of some high performance compressors.

Thus, running the compressor at maximum performance risks entering a stall cycle under any small disturbance. Several feedback designs to stabilize surge and stall through varying throttle opening γ have appeared in the literature beginning with [13]. The result in Reference [14] reduced the sensing requirement for global asymptotic stabilization (GAS) from three to two (Ψ and Φ) measurements; in Reference [15], an output feedback controller achieves semi-global stabilization using only pressure sensing, and most recently, the result in Reference [16] achieves GAS using only pressure (Ψ) measurement. In Reference [17], extremum seeking feedback was used in an experiment to optimize performance of a compressor stabilized by air-injection; this led to less demanding sensing and actuation requirements than stabilization of stalled equilibria. The result in Reference [18] derives geometric sufficient conditions for stabilization of the bifurcations for use in low spatial actuation authority schemes.

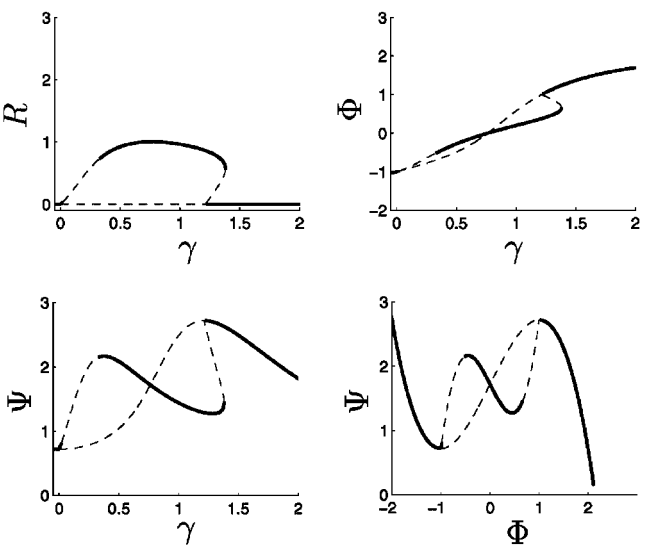

Figure 6. Bifurcation diagrams for the open-loop system with $\varepsilon = 0$ and $\beta = 0.71$. The throttle opening γ is the bifurcation parameter.

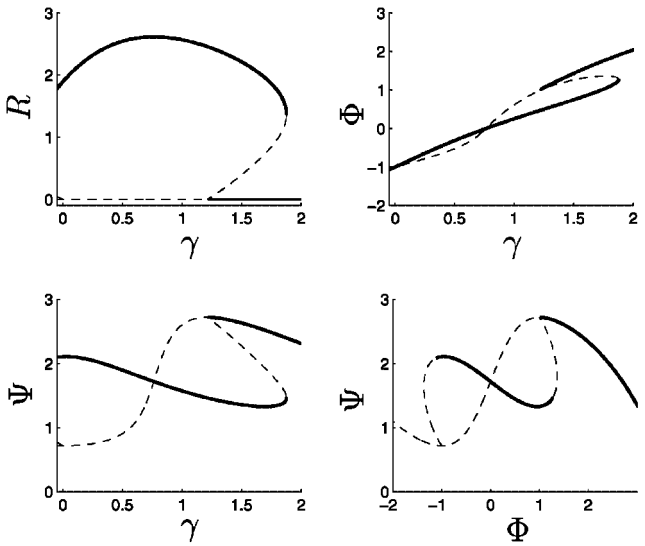

Figure 7. Bifurcation diagrams for the open-loop system with $\varepsilon = 0.9$ and $\beta = 0.71$. The throttle opening γ is the bifurcation parameter.

Here, we illustrate achievement of near-optimal performance of the compressor under slope-seeking feedback that uses only the pressure measurement Ψ, and actuates throttle opening γ. Through slope seeking, we can operate at a point on the compressor characteristic that is just short of the maximum. This is done by using a slope setting $r(f'_{\text{ref}})$ with commanded slope f'_{ref} small and negative in the slope seeking scheme (Figure 1).

Slope seeking design: We design two slope seeking loops; one for the case of low hysteresis, $\varepsilon = 0$, and for the case of deep hysteresis, $\varepsilon = 0.9$. In both designs, we choose forcing frequency $\omega = 0.5$, forcing amplitude $a = 0.025$, gain $k = -0.6$, and pole of washout filter $h = 0.5$. We set commanded slopes $f'_{\text{ref}} = -0.9$ and -0.5 for the $\varepsilon = 0$ and 0.9 cases, respectively, obtaining values of $r(f'_{\text{ref}}) = -af'_{\text{ref}}/2\,\text{Re}\{\text{j}\omega/(\text{j}\omega + h)\} = 0.0056, 0.0031$ for the slope settings neglecting plant dynamics.

Simulation results: We perform simulations** with low performance initial conditions of $R(0) = 1$, $\Phi(0) = 1.8565$, $\Psi(0) = 1.3055$, $\gamma(0) = 1.5$ for the $\varepsilon = 0$ case, and initial conditions of $R(0) = 1$, $\Phi(0) = 1.4877$, $\Psi(0) = 1.9463$, $\gamma(0) = 1.5$ for the $\varepsilon = 0.9$ case. Figures 8 and 9 show the results for slope seeking (solid lines) along with results for extremum seeking, $r = 0$ (in dotted lines) for the initial conditions above. The results reveal the following features:

1. Both slope seeking and extremum seeking converge to their desired set points: extremum seeking to the maximum pressure, and slope seeking to a point slightly below the maximum.

**All simulations were performed in MATLAB and SIMULINK.

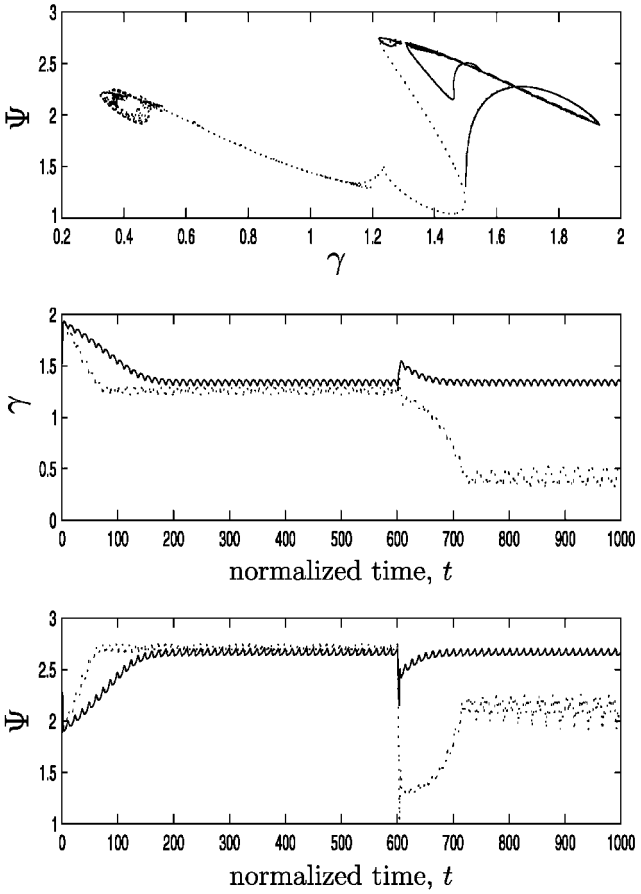

Figure 8. Low hysteresis compressor: $\varepsilon = 0$.

2. Under a small disturbance at $t = 600$, the system with extremum seeking is destabilized and the system goes into the stall regime, while slope seeking feedback recovers its performance.

APPENDIX A: LEMMAS

Lemma A1

If the transfer function $H(s)$ has all of its poles with negative real parts, then for any real ψ,

$$H(s)[\sin(\omega t - \psi)] = \mathrm{Im}\{H(\mathrm{j}\omega)\mathrm{e}^{\mathrm{j}(\omega t - \psi)}\} + \varepsilon^{-t} \tag{A1}$$

where ε^{-t} denotes exponentially decaying terms.

This is simply the frequency response of an asymptotically stable LTI system.

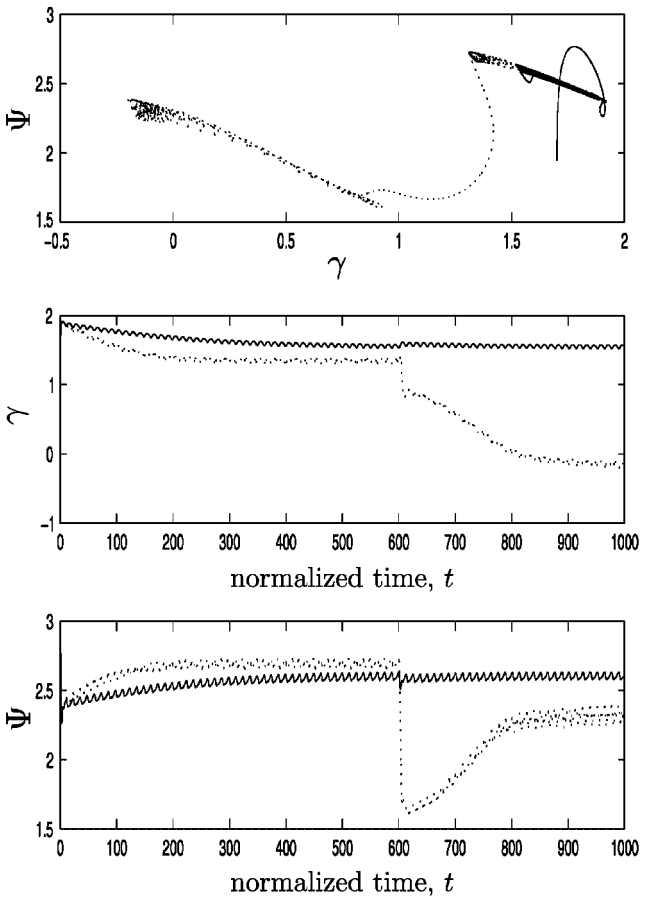

Figure 9. Deep hysteresis compressor: $\varepsilon = 0.9$.

Lemma A2

For any two rational functions $A(\cdot)$ and $B(\cdot\,,\cdot)$, the following is true:

$$\begin{aligned}&\mathrm{Im}\{\mathrm{e}^{\mathrm{j}(\omega_a t-\psi)}A(\mathrm{j}\omega_a)\}\ \mathrm{Im}\{\mathrm{e}^{\mathrm{j}(\omega_b t-\phi)}B(s,\mathrm{j}\omega_b)[z(t)]\}\\ &\quad=\tfrac{1}{2}\,\mathrm{Re}\{\mathrm{e}^{\mathrm{j}((\omega_b-\omega_a)t+\psi-\phi)}A(-\mathrm{j}\omega_a)B(s,\mathrm{j}\omega_b)[z(t)]\}\\ &\quad-\tfrac{1}{2}\,\mathrm{Re}\{\mathrm{e}^{\mathrm{j}((\omega_b+\omega_a)t-\psi-\phi)}A(\mathrm{j}\omega_a)B(s,\mathrm{j}\omega_b)[z(t)]\}\end{aligned}$$

Proof

Follows by substituting the representations for the real and imaginary parts of a complex number z, $\mathrm{Re}\{z\} = (z+\bar{z})/2$, and $\mathrm{Im}\{z\} = (z-\bar{z})/2$.

Lemma A3 (Singular perturbation)
Consider the singularly perturbed system given by the equations:

$$\dot{\mathbf{x}} = \mathbf{A}_1(t)\mathbf{x} + \mathbf{B}_1(t)\mathbf{u}, \quad \mathbf{x}(t_0) = \xi(\varepsilon)$$

$$\mathbf{v} = \mathbf{C}_1(t)\mathbf{x} \tag{A2}$$

$$\varepsilon\dot{\mathbf{z}} = \mathbf{A}_2\mathbf{z} + \mathbf{B}_2\mathbf{v}, \quad \mathbf{z}(t_0) = \eta(\varepsilon)$$

$$\mathbf{u} = \mathbf{C}_2\mathbf{z} \tag{A3}$$

where $\xi(\varepsilon)$ and $\eta(\varepsilon)$ are smooth functions of ε. If $\mathbf{A}_2$ is Hurwitz and the origin of the reduced LTV model

$$\dot{\bar{\mathbf{x}}} = (\mathbf{A}_1(t) + \mathbf{B}_1(t)\mathbf{C}_2\mathbf{A}_2^{-1}\mathbf{B}_2\mathbf{C}_1(t))\bar{\mathbf{x}} \tag{A4}$$

is exponentially stable, then there exists $\varepsilon^* > 0$ such that for all $0 < \varepsilon < \varepsilon^*$, the system in Equations (A2) and (A3) has a unique solution $\mathbf{x}(t,\varepsilon)$, $\mathbf{z}(t,\varepsilon)$ defined for all $t \geqslant t_0 \geqslant 0$ and $\mathbf{x}(t,\varepsilon) - \bar{\mathbf{x}}(t) = O(\varepsilon)$.

Proof

A direct consequence of Theorem 9.4 in Reference [12].

ACKNOWLEDGEMENTS

This work was supported in part by grants from AFOSR, ONR and NSF.

REFERENCES

1. Ariyur KB, Krstic M. Multiparameter extremum seeking. Revised and resubmitted to *IEEE Transactions on Automatic Control*, March 2003.
2. Krstic M. Performance improvement and limitations in extremum seeking control. *Systems and Control Letters* 2000; **39**:313–326.
3. Krstic M, Wang H-H. Stability of extremum seeking feedback for general nonlinear dynamic systems. *Automatica* 2000; **36**:595–601.
4. Rotea MA. Analysis of multivariable extremum seeking algorithms. *Proceedings of the American Control Conference*, Chicago, IL, June 2000; 433–437.
5. Teel AR, Popovic D. Solving smooth and nonsmooth multivariable extremum seeking problems by the methods of nonlinear programming. *Proceedings of the American Control Conference*, Arlington, VA, June 2001; 2394–2399.
6. Walsh GC. On the application of multi-parameter extremum seeking control. *Proceedings of the American Control Conference*, Chicago, IL, June 2000; 411–415.
7. Wang H-H, Krstic M, Larsen M. Control of deep hysteresis aeroengine compressors. *Journal of Dynamic Systems, Measurement, and Control* 2000; **122**:140–152.
8. Tunay I. Antiskid control for aircraft via extremum seeking. *Proceedings of the American Control Conference*, Arlington, VA, June 2001; 665–670.
9. Binetti P, Ariyur KB, Krstic M, Bernelli F. Formation flight optimization using extremum seeking feedback. *AIAA Journal of Guidance, Control, and Dynamics* 2003; **26**(2):132–142.
10. Hui W, Bamieh BA, Miley GH. Robust burn control of a fusion reactor by modulation of the refueling rate. *Fusion Technology* 1994; **25**:318–325.
11. Moore FK, Greitzer EM. A theory of post-stall transients in axial compression systems—Part I: development of equations. *Journal of Engineering for Gas Turbines and Power* 1986; **108**:68–76.

12. Khalil HK. *Nonlinear Systems*. Prentice-Hall: Upper Saddle River, NJ, 1996.
13. Liaw D-C, Abed EH. Active control of compressor stall inception: a bifurcation theoretic approach. *Automatica* 1996; **32**:109–115.
14. Krstić M, Fontaine D, Kokotović PV, Paduano JD. Useful nonlinearities and global bifurcation control of jet engine surge and stall. *IEEE Transactions on Automatic Control* 1998; **43**:1739–1745.
15. Isidori A. *Nonlinear Control Systems*, vol. II. Springer: London, UK, 2000.
16. Arcak M, Kokotovic PV. Nonlinear observers: a circle criterion design and robustness analysis. *Automatica* 2001; **37**:1923–1930.
17. Wang H-H, Yeung S, Krstic M. Experimental application of extremum seeking on an axial-flow compressor. *IEEE Transactions on Control Systems Technology* 2000; **8**:300–309.
18. Wang Y, Murray RM. A geometric perspective on bifurcation control. *Proceedings of the 39th IEEE Conference on Decision and Control*, Sydney, Australia, December 2000; 1613–1618.

